NONLINEAR WAVE LOADING USING SIGMA-TRANSFORMED AND UNSTRUCTURED FINITE ELEMENT MESHING

A G L Borthwick, M S Turnbull & R Eatock Taylor
Department of Engineering Science, Oxford University, Parks Road, Oxford OX1 3PJ, U.K.

ABSTRACT

This paper describes a finite element numerical scheme for modelling the wave-induced loading on a horizontal cylinder. A numerical wave tank is utilised with a σ-transformation applied to regions upwave and downwave of the cylinder in order to take advantage of the mapping between free surface and bed. The region around the cylinder is discretised using a Voronoi mesh, with free surface tracking achieved using the Wu and Eatock Taylor (1994) scheme. In this case, the free surface velocities are determined using an accurate higher order interpolation scheme. A combination of the Sommerfeld radiation condition and a damping zone is used to eliminate end effects at the far radiation boundary. Results are presented for sloshing free surface motions in a rectangular tank, progressive waves with and without an immersed horizontal cylinder. Promising agreement is achieved with the analytical and experimental force data of Ogilvie (1963) and Chaplin (1984).

INTRODUCTION

For offshore structures subject to loading in the inertial regime, fully nonlinear potential theory is necessary for predicting relatively large free surface or body motions. Whereas first and second order potential theories have been developed for small amplitude motions, the effects of higher order nonlinearity become increasingly evident in steep waves or where body motions are significant. Wu and Eatock Taylor (1995) have demonstrated that the finite element method can be substantially more efficient than the boundary element method for solving such problems. This is because, although the finite element method involves discretising the entire domain unlike the boundary element method, savings can be made because the finite element matrix is sparsely populated and the coefficients are straightforward to determine. The present paper describes a continuation of the Wu and Eatock Taylor model, whereby a σ-transformation is used to stretch the mesh linearly between the bed and free surface in regions where the fluid is continuous and there is a unique mapping between the bed and free surface. In other regions where for example a horizontal cylinder is situated, Wu and Eatock Taylor's (1995) finite element solver is used with an unstructured Voronoi mesh fitted to the problem boundaries. In the former case, the mapping inherently takes care of the moving boundary. In the latter, the free surface is moved forward in time by calculating the displacements according to the surface velocity components.

MATHEMATICAL FORMULATION

Consider a two-dimensional free surface flow of an incompressible inviscid fluid without surface tension. We assume the flow is irrotational, and potential theory applies whereby the velocity vector **u** is related to the velocity potential ϕ by $\mathbf{u} = \nabla\phi$. Invoking irrotationality, $\nabla^2\phi = 0$ throughout the fluid domain. The boundary conditions are as follows: $\dfrac{\partial\phi}{\partial n} = 0$ at all solid surfaces; $\dfrac{\partial\phi}{\partial x} = U(t)$ at the wave-maker where $U(t)$ is the wave-maker velocity at time *t*; the kinematic free surface boundary conditions $\dfrac{\mathrm{D}x}{\mathrm{D}t} = \dfrac{\partial\phi}{\partial x}$ and $\dfrac{\mathrm{D}z}{\mathrm{D}t} = \dfrac{\partial\phi}{\partial z}$, and dynamic free surface boundary condition $\dfrac{\mathrm{D}\phi}{\mathrm{D}t} - \dfrac{1}{2}\left|\nabla\phi\right|^2 + gz = 0$ at $z = \zeta(x,t)$.

FINITE ELEMENT FORMULATION

Multiplying Laplace's equation by linear shape functions, $N_j(x,z)$, such that $\phi = \sum_{j=1}^{n} \phi_j N_j(x,z)$ and integrating over the domain, Wu & Eatock Taylor (1995) derived

$$\int_S N_i \frac{\partial\phi}{\partial n}\,\mathrm{d}S - \int_R \nabla N_i \cdot \nabla\phi \;\mathrm{d}R = 0 \quad .$$

Replacing ϕ with its approximation and the potential derivative with f_2, gives

$$\int_R \nabla N_i \cdot \sum_{j=1}^{n} \phi_j \nabla N_j \, \mathrm{d}R \Bigg|_{j \notin S_1} = -\int_R \nabla N_i \cdot \sum_{j=1}^{n} \phi_j \nabla N_j \, \mathrm{d}R \Bigg|_{j \in S_1} + \int_{S_2} N_i f_2 \, \mathrm{d}S$$

in which S_1 is the boundary where the velocity potential is specified, and S_2 is the boundary where the normal derivative of the velocity potential, f_2, is known. In matrix form, this may be written $[A]\{\phi\} = \{B\}$ where $A_{ij} = \int_R \nabla N_i \cdot \nabla N_j \mathrm{dR}$ or $A_{ij} = 1$ if $i = j$ and $i \in S_1$ or $A_{ij} = 0$ if $i \in S_1$ or $j \in S_1$ and $i \neq j$, and $B_i = -\int_R \nabla N_i \cdot \sum_{j=1}^{n} \phi_j \nabla N_j \mathrm{dR} \Big|_{j \in S_1} + \int_{S_2} N_i f_2 \mathrm{dS}$ or $B_i = \phi_i$ if $i \in S_1$.

SIGMA-TRANSFORMED FORMULATION

We choose stretched co-ordinates between the bed and free surface such that $X = \frac{x}{l}$, $\sigma = \frac{z+d}{h}$ and $T = t$, where l is the length of the domain, d is the still water depth and h is the total water depth ($h = d + \eta$). Using the chain rule: $\frac{\partial}{\partial x} = \frac{1}{l}\frac{\partial}{\partial X} + \left(\frac{\partial \sigma}{\partial x}\right)\frac{\partial}{\partial \sigma}$; $\frac{\partial}{\partial z} = \frac{1}{h}\frac{\partial}{\partial \sigma}$; and $\frac{\partial}{\partial t} = \frac{\partial}{\partial T} + \left(\frac{\partial \sigma}{\partial T}\right)\frac{\partial}{\partial \sigma}$. In the σ-transformed system, $\mathrm{d}R = \mathrm{d}x\mathrm{d}z = lh\mathrm{d}X\mathrm{d}\sigma$, and $\nabla = \begin{pmatrix} \frac{\partial}{\partial x} \\ \frac{\partial}{\partial z} \end{pmatrix} = \begin{pmatrix} \frac{1}{l}\frac{\partial}{\partial X} + \left(\frac{\partial \sigma}{\partial x}\right)\frac{\partial}{\partial \sigma} \\ \frac{1}{h}\frac{\partial}{\partial \sigma} \end{pmatrix}$. The general form of a linear shape function is $N_i = (\alpha_i + \beta_i X + \gamma_i \sigma)/2\Delta$ where $\alpha_1 = X_2\sigma_3 - X_3\sigma_2$, $\alpha_2 = X_3\sigma_1 - X_1\sigma_3$, $\alpha_3 = X_1\sigma_2 - X_2\sigma_1$, $\beta_1 = \sigma_2 - \sigma_3$, $\beta_2 = \sigma_3 - \sigma_1$, $\beta_3 = \sigma_1 - \sigma_2$, $\gamma_1 = X_3 - X_2$, $\gamma_2 = X_1 - X_3$, $\gamma_3 = X_2 - X_1$, and Δ is the area of the element. The spatial derivatives of the shape functions become $\frac{\partial N_i}{\partial X} = \frac{\beta_i}{2\Delta}$ and $\frac{\partial N_i}{\partial \sigma} = \frac{\gamma_i}{2\Delta}$. Therefore over a particular element,

$$\nabla N_i \cdot \nabla N_j = \frac{1}{l^2}\frac{\beta_i \beta_j}{4\Delta^2} + \frac{1}{l}\left(\frac{\partial \sigma}{\partial x}\right)\frac{(\beta_i \gamma_j + \beta_j \gamma_i)}{4\Delta^2} + \left(\frac{\partial \sigma}{\partial x}\right)^2 \frac{\gamma_i \gamma_j}{4\Delta^2} + \frac{1}{h^2}\frac{\gamma_i \gamma_j}{4\Delta^2}.$$

Integrating over the element,

$$\frac{1}{l}\frac{\beta_i \beta_j}{4\Delta^2}\int_e h\mathrm{d}X\mathrm{d}\sigma + \frac{(\beta_i \gamma_j + \beta_j \gamma_i)}{4\Delta^2}\int_e \left(\frac{\partial \sigma}{\partial x}\right) h\mathrm{d}X\mathrm{d}\sigma + \frac{l\gamma_i \gamma_j}{4\Delta^2}\int_e \left(\frac{\partial \sigma}{\partial x}\right)^2 h\mathrm{d}X\mathrm{d}\sigma + \frac{l\gamma_i \gamma_j}{4\Delta^2}\int_e \frac{1}{h}\mathrm{d}X\mathrm{d}\sigma$$

The integral expressions are evaluated using cubic formulae, and the matrix equation solved by Gaussian elimination.

VELOCITY CALCULATION

The velocity components are $u = \frac{\partial \phi}{\partial x} = \frac{1}{l}\frac{\partial \phi}{\partial X} + \frac{1}{lh}\left(-\sigma \frac{\partial \eta}{\partial X} + (1-\sigma)\frac{\partial d}{\partial X}\right)\frac{\partial \phi}{\partial \sigma}$ and $w = \frac{\partial \phi}{\partial z} = \frac{1}{h}\frac{\partial \phi}{\partial \sigma}$. At the free surface, the velocity components are used to estimate rates of change of free surface elevation and velocity potential with time. The σ-transformed free surface kinematic boundary condition gives $\frac{\partial \eta}{\partial t} = w - u\frac{\partial \eta}{\partial x} = w - \frac{u}{l}\frac{\partial \eta}{\partial X}$. For a uniform sea bed, $\frac{\partial \sigma}{\partial t} = -\frac{\sigma}{l}\frac{\partial \eta}{\partial t}$, and so $\frac{\partial \Phi}{\partial T} = \frac{\partial \Phi}{\partial t} + \frac{\sigma}{h}\frac{\partial \eta}{\partial t}\frac{\partial \Phi}{\partial \sigma} = \frac{\partial \Phi}{\partial t} + \sigma \frac{\partial \eta}{\partial t}\frac{\partial \Phi}{\partial z}$. At the free surface, $\sigma = 1$, and the dynamic free surface

boundary condition gives, $\frac{\partial \Phi}{\partial T} = -g\eta - \frac{\left(u^2 + w^2\right)}{2} + \frac{\partial \eta}{\partial T} w$. A fourth-order Runge-Kutta scheme is used to step free surface elevation and potential forward in time.

RESULTS

Sloshing in a Fixed Rectangular Tank

Here, a tank of length twice that of the still water depth is considered. The initial elevation is sinusoidal such that one wavelength fits the tank. Almost exact agreement was obtained with Wu and Eatock Taylor's (1994) second order analytical solution when the wave amplitude to depth ratio a/d = 0.001. Fig.1 depicts the time history of the free surface at the tank centre for a wave of greater amplitude a/d = 0.1. The results from both the σ-transformed and Wu and Eatock Taylor (1995) schemes are almost identical. The effect of higher order wave nonlinearity is evident with a phase shift evident and higher free surface maxima than for the second order potential solution. The effect of nonlinearity can also be seen in Fig. 2 which shows the free surface profile along the tank at different times during a cycle. There is a narrower central peak and wider trough than for a linear sinusoidal standing wave. The fixed positions of nodes that exist for small amplitude cases are not present here. These results are in close agreement with those of Chern *et al*. (1999). Fig. 3 depicts the spatial free surface profiles along the tank for a relatively large amplitude case (a/d = 0.05) where the wavelength of the initial sinusoidal free surface elevation is half the length of the tank. Again, the crests are clearly sharper and troughs shallower than for linear sinusoidal motions.

Sloshing in a Base-excited Tank

Wu *et al*. (1998) gave the linear solution for free surface motions of inviscid liquid in a tank where the base was oscillated horizontally. Fig. 4 illustrates the very close agreement between the finite element model predictions and the analytical solution for a near resonant case, where the excitation frequency $\omega = 1.1\omega_o$ (and ω_o is the natural sloshing frequency of the tank). The finite element scheme predicts increasingly higher peaks than the analytical model as the initial oscillations grow in amplitude; this is again due to high order nonlinearity.

Regular Waves

Progressive waves were generated by imposing the linear theory horizontal velocity distribution at the left hand boundary of the domain. The velocity amplitude was ramped up over a predetermined period to avoid spurious oscillations. At the right hand end of the tank, wave absorption was achieved using a combination of the Sommerfeld radiation condition with a damping zone. Fig. 5 represents the free surface evolution along the tank with time, whereby spatial profiles are plotted at time intervals of twice the wave period. The overlaid plots demonstrate the repeatability of the wave generation process. The first and second order components of waves of steepness ka up to 0.194, were found to be almost identical to analytical values from Stokes' second order theory.

Horizontal Cylinder Under Regular Waves

In order to insert a horizontal cylinder in the wave tank, a combination of structured and unstructured finite element meshes was used. A typical example of the unstructured region is shown in Fig. 6. The total force may be calculated by integrating the surface pressure profile around the cylinder. The first and second order force components in the vertical and horizontal directions were determined using Fourier analysis. Reasonable agreement is obtained with Ogilvie's (1963) semi-analytical model and Chaplin's (1984) experimental data, as the following example illustrates. For a non-dimensional wave frequency ω =1.8495, non-dimensional depth of immersion $d_c = 0.18$, and non-dimensional cylinder radius A = 0.06, Ogilvie predicts $\left|F^{(1)}\right| / A = 0.0430$, Chaplin obtains $\left|F^{(1)}\right| / A = 0.0415$, whereas the present scheme predicts $\left|F_x^{(1)}\right| / A = 0.0435$ and $\left|F_z^{(1)}\right| / A = 0.0429$. Moreover, for the second order mean vertical force, $\overline{F_z^{(2)}} / A^2$, the corresponding results from Ogilvie, Chaplin and the present scheme are 0.0914, 0.0944 and 0.0930, respectively.

CONCLUSIONS

A numerical wave tank has been described based on finite element models with σ-transformed and unstructured mesh systems. Simulations of nonlinear sloshing waves in fixed and base-excited tanks

have been found to agree well with analytical solutions, and the numerical results of Chern *et al.* (1999). Progressive regular waves have been simulated in close agreement with Stokes' second order theory. Sensible estimates have been made of the first and second order forces on a submerged horizontal cylinder under waves, in comparison with Ogilvie (1963) and Chaplin (1984).

REFERENCES

Chaplin, J.R. (1984) "Nonlinear forces on a horizontal cylinder beneath waves", J. Fluid Mech., 147: 449-464.

Chern, M.J., Borthwick, A.G.L., and Eatock Taylor (1999) "A pseudospectral σ-transformation model of 2-D nonlinear waves", Journal of Fluids and Structures, 13: 607-630.

Ogilvie, T.F. (1963) "First- and second-order forces on a cylinder submerged under a free surface", J. Fluid Mech., 16: 451-472.

Wu, G.X., and Eatock Taylor, R. (1994) "Finite element analysis of two-dimensional nonlinear transient water waves", Appl. Ocean Res., 16: 363-372.

Wu, G.X., and Eatock Taylor, R. (1995) "Time stepping solutions of the two-dimensional non-linear wave radiation problem", Ocean Eng., 22(8): 785-798.

Wu, G.X., Ma, Q.W., and Eatock Taylor, R. (1998) "Numerical simulation of sloshing waves in a 3D tank based on a finite element method", Appl. Ocean Res., 20: 337-355.

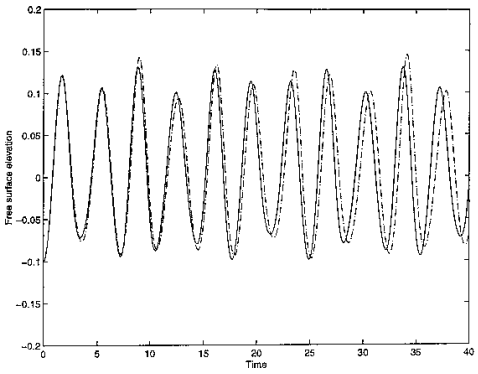

Fig.1 Free surface motions at tank centre

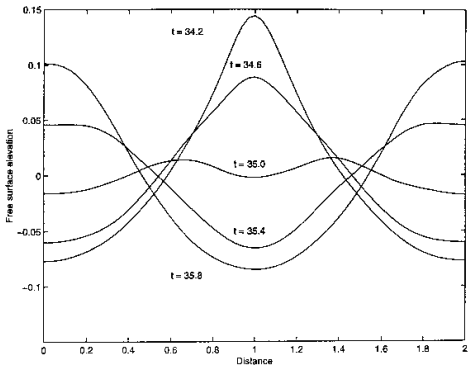

Fig.2 Wave profiles: $a = 0.1$

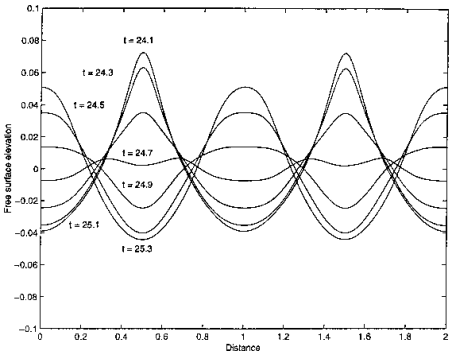

Fig. 3 Double standing wave profiles: $a = 0.05$

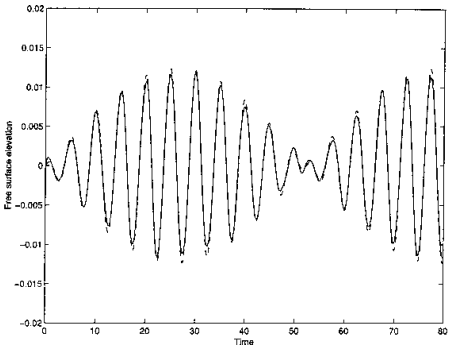

Fig.4 Free surface motions at left wall: Base-excited tank: $\omega = 1.1\,\omega_o$

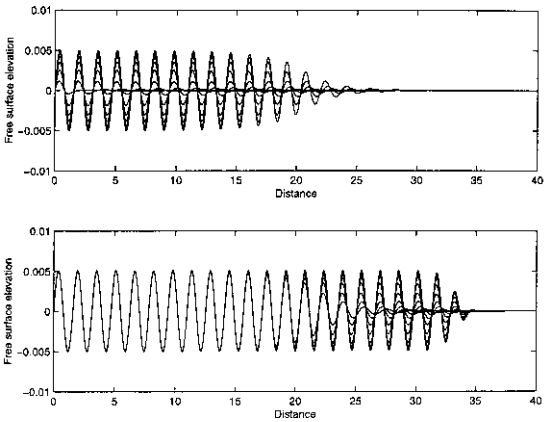

Fig. 5 Evolution of regular waves

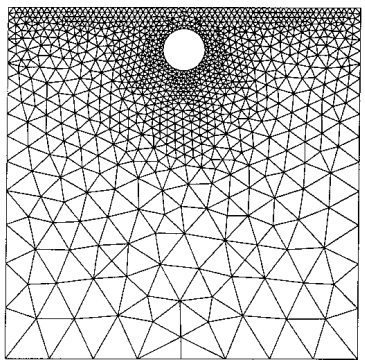

Fig. 6 Voronoi mesh about cylinder